

On the numerical evaluation of real-time path integrals: Double exponential integration and the Maslov correction

R. Rosenfelder

Particle Theory Group, Paul Scherrer Institute, CH-5232 Villigen PSI, Switzerland

Abstract

Ooura's double exponential integration formula for Fourier transforms is applied to the oscillatory integrals occurring in the path-integral description of real-time Quantum Mechanics. Due to an inherent, implicit regularization multi-dimensional Gauss-Fresnel integrals are obtained numerically with high precision but modest number of function calls. In addition, the Maslov correction for the harmonic oscillator is evaluated numerically with an increasing number of time slices in the path integral thereby clearly demonstrating that the real-time propagator acquires an additional phase $-\pi/2$ each time the particle passes through a focal point. However, in the vicinity of these singularities an overall small damping factor is required. Prospects of evaluating scattering amplitudes of finite-range potentials by direct numerical evaluation of a real-time path integral are discussed.

1. Introduction

Among the many formulations of Quantum Mechanics the path-integral method (see e.g. [1], [2], [3]) is a very attractive one as it gives rise to new insights, approximation schemes and can be readily generalized to Many-Body Physics and Quantum Field Theory. However, for numerical evaluation a path (i.e. functional, i.e. infinite-dimensional) integral poses an extraordinary challenge requiring at present (unphysical) imaginary time and Monte-Carlo methods. Still, due to the heavy oscillations of the integrand in real time scattering cannot be treated in this way (apart from low-energy quantities) and one has to resort to semi-classical approximative methods (see, e.g. Ref. [6]).

In a broader context "numerical integration" is essential in all quantitative sciences, not only in theoretical and computational physics. It is "a wide field" [4] with a vast literature which cannot be cited adequately here (a standard textbook is Ref. [5]) and many different methods.

It is somehow surprising that after centuries of work on numerical integration rules (associated with the names of Kepler, Newton, Simpson, Lagrange, Gauss and others) a new contender for the "best" all-purpose method appeared: the double exponential (DE) integration (or tanh-sinh quadrature) method of Takahasi and Mori [7] (see also Ref. [8]). This method has become a standard tool to obtain high-precision results with only $\mathcal{O}(N \ln N)$ function calls [9]. This is due to a transformation $x = \phi(t)$ which maps a finite interval into an infinite one and leads to a new integrand which decays asymptotically with double exponential rate so that the integral can be best approximated by the extended trapezoidal rule. Although other integration schemes (like Gaussian quadrature) are superior for smooth integrands, it can be argued that the DE-method comes close to a all-purpose quadrature scheme ¹.

Ooura and Mori [10] have extended this scheme to oscillating integrands and found spectacular results. For example, Euler's constant is obtained from integrating

$$\int_0^{\infty} dx (-\ln x) \sin x = \gamma_E \tag{1.1}$$

to an absolute accuracy of 10^{-12} with only 80 function calls (see Table 2 in Ref. [10]) despite the fact that the integral only exists as limiting case

$$\lim_{\eta \rightarrow 0} \int_0^{\infty} dx (-\ln x) \sin x e^{-\eta x} . \tag{1.2}$$

Thus the double exponential method implicitly introduces a suitable regularization scheme. This makes it a very appealing quadrature rule for quantum-mechanical path integrals in real time

$$\int \mathcal{D}x(t) \exp \left\{ i \int_{t_a}^{t_b} dt \left[\frac{m}{2} \dot{x}^2(t) - V(x(t)) \right] \right\} \tag{1.3}$$

where the convergence of these (Fresnel-type) integrals is ensured by Feynman's " $i0^+$ -rule" which either modifies the mass $m \rightarrow m + i0^+$ or the squared frequency in a harmonic oscillator potential $V = m\Omega^2 x^2/2$ as $\Omega^2 \rightarrow \Omega^2 - i0^+$. As a free field theory can be seen as a system of coupled oscillators it is not surprising that the latter prescription (here for the squared mass) is needed to specify the singularities of Green functions.

It is the purpose of this work to show that a direct evaluation of multi-dimensional oscillating integrals is possible by applying the double exponential methods alluded to before. This will be demonstrated by calculating high-dimensional Gauss-Fresnel integrals and by evaluating the so-called Maslov phase for a non-relativistic particle in a harmonic oscillator well where the exact solutions are readily available.

¹A caveat: in certain applications the method fails to give accurate results [11]. This is not surprising as realistically one may doubt whether a "best" scheme for *all* functions exists .

2. Double exponential integration

Ooura and Mori use a transformation $\phi(t)$ such that the derivative $\phi'(t)$ goes to zero double exponentially for $t \rightarrow -\infty$ while the function $\phi(t)$ approaches t double exponentially as $t \rightarrow +\infty$. The latter property ensures that for large t the zeroes of the oscillating integrand are nearly hit leading to the fast convergence of the scheme.

Ooura has later given an improved version of this method ² which I will use in the following, viz. "Approximation formula 2" (Eq. (3.5) in Ref.[13]) with the simplifications $\omega_0 = \omega$ and $N_+ = N_- \equiv k_{\max}$. Although originally only given for $\omega > 0$ one can extend it also to the case $\omega < 0$ by complex conjugation provided the function $f(x)$ is real. Thus

$$\int_0^\infty dx f(x) e^{i\omega x} \simeq \frac{\pi}{|\omega|} \sum_{k=-k_{\max}}^{k=+k_{\max}} f\left(\frac{\pi}{|\omega|h} \phi(kh)\right) \phi'(kh) \left\{ \exp\left[i \operatorname{sgn}(\omega) \frac{\pi}{h} \phi(kh)\right] - (-1)^k \right\} \quad (2.1)$$

where $\operatorname{sgn}(\omega) := \omega/|\omega|$ and

$$\phi(t) = \frac{t}{1 - \exp[-2t - \alpha(1 - e^{-t}) - \beta(e^t - 1)]}. \quad (2.2)$$

Ooura's parameter α, β are ω -dependent:

$$\beta = \frac{1}{4}, \quad 0 < \alpha = \beta \sqrt{\frac{4|\omega|h}{4|\omega|h + \ln\left(1 + \frac{\pi}{|\omega|h}\right)}} < \beta. \quad (2.3)$$

Note that the case $\omega = 0$ is undefined in Ooura's integration rule although one would then expect that it reduces to the standard double exponential integration rule for an half-infinite interval. However, questions about the allowed frequency range or the class of admissible functions are outside the scope of the present work.

3. Application I: Multi-dimensional Gauss-Fresnel integral

I define the simplest N -dimensional Gauss-Fresnel integral as

$$GF_N(\omega) := \int d^N y \exp\left(i\omega \sum_{k=1}^N y_k^2\right), \quad \omega \text{ real}. \quad (3.1)$$

Its analytical value is obtained by a regularization

$$GF_N(\omega) = \lim_{\eta \rightarrow 0} \prod_{k=1}^N \left(\int d^N y \exp[i(\omega + i\eta)y^2] \right) = \lim_{\eta \rightarrow 0} \left(\frac{\pi i}{\omega + i\eta} \right)^{N/2} = \left(\frac{\pi}{|\omega|} \right)^{N/2} \exp\left(i \operatorname{sgn}(\omega) \pi \frac{N}{4}\right) \quad (3.2)$$

where the positive sign of the square root has to be taken (for a thorough mathematical treatment see, e.g. Refs. [14], [15]).

I will calculate the Gauss-Fresnel integral in *hyperspherical co-ordinates*. As the integrand only depends on the hyperradius $R = (\sum_{k=1}^N y_k^2)^{1/2}$ one obtains

$$GF_N(\omega) = S_{N-1} \cdot \int_0^\infty dR R^{N-1} \exp(i\omega R^2) \quad (3.3)$$

²See Fig. 3 in Ref. [12] for a comparison with the old method for the integral in Eq. (1.1).

where

$$S_{N-1} = \frac{2\pi^{N/2}}{\Gamma(N/2)} \quad (3.4)$$

is the $(N - 1)$ -dimensional surface of the N -sphere. The variable change $R = \sqrt{y}$ brings the integral into the form

$$GF_N(\omega) = \frac{1}{2} S_{N-1} \int_0^\infty dy y^{N/2-1} e^{i\omega y} \quad (3.5)$$

to which Oura's numerical integration formula (2.1) will be applied. Note that this application is much more demanding than the numerical evaluation of Euler's number by Eq. (1.1) as now the integrand grows power-like instead of logarithmically.

Fig. 1 shows how much the numerical result (for $\omega = \pm 1$) deviates from the exact one. Here and in the following I use as metric the "relative complex deviation"

$$\delta_{\text{rel}}[GF] := \left| \frac{GF_{\text{num}} - GF_{\text{exact}}}{GF_{\text{exact}}} \right| \quad (3.6)$$

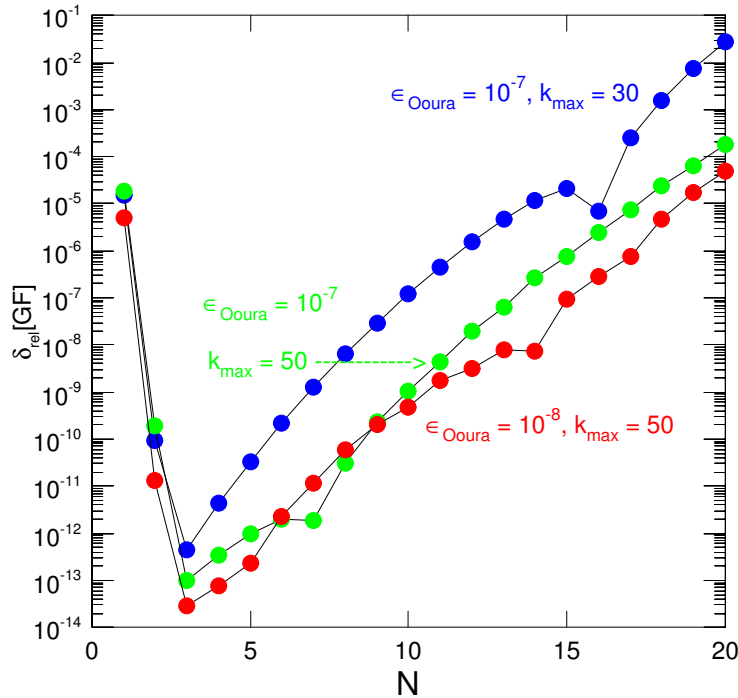


Fig. 1 : Relative complex deviation (as defined in Eq. (3.6)) of the Gauss-Fresnel integral evaluated numerically with Oura's method from the exact value for $\omega = \pm 1$ and increasing dimension N . Results for different accuracy parameters (see Table 1) are depicted.

which quantifies the agreement of the numerical calculation compared with the exact result both for the absolute magnitude as for the phase of a complex quantity. Obviously a very good agreement with the exact values is obtained in a wide range of dimensions – without any regularization!

4. Application II: Maslov correction for the harmonic oscillator

It is long known [16] and covered in many textbooks (e.g. in Ref. [17], ch. 17 or Ref. [2], p. 100) but frequently overseen ³ that the matrix element of the time-evolution operator for a non-relativistic particle in a harmonic potential

$$V^{\text{h.o.}}(x) = \frac{m}{2}\Omega^2 x^2 \quad (4.1)$$

as given by

$$\langle x_b | \hat{U}^{\text{h.o.}}(t_b, t_a) | x_a \rangle = F^{\text{h.o.}}(T = t_b - t_a) \cdot \exp [iS_{\text{class}}^{\text{h.o.}}(x_b, x_a; T)] \quad (4.2)$$

acquires an additional phase each time the particle passes through a *focal point* at $\Omega T = n\pi$ with $n = 1, 2, \dots$. In Eq. (4.2) $S_{\text{class}}^{\text{h.o.}}(x_b, x_a; T)$ is the classical action of the harmonic oscillator (for an explicit expression see, e.g. eq. (1.64) in Ref. [3]) and

$$F^{\text{h.o.}}(T) = \left(\frac{m\Omega}{2\pi i |\sin(\Omega T)|} \right)^{d/2} e^{-\frac{1}{2}i\pi d n_M}, \quad n_M = \sum_{n=1}^{\infty} \Theta(\Omega T - n\pi) \quad (4.3)$$

the prefactor in d space dimensions which is due to the quantum fluctuations ($\Theta(x)$ is the step or Heaviside function and a system of units is used in which $\hbar = 1$). Obviously, the prefactor diverges at these focal points (creating the so-called caustics) and the particle starts anew its quantum-mechanical propagation (like "a phoenix rising from the ashes") but with an additional phase $-\pi/2$ as sole remainder of its previous history.

It should be emphasized that the Maslov correction is a genuine quantum-mechanical phenomenon occurring only in real time: The euclidean version (for example the partition function) does not display it ⁴. The occurrence of the Maslov correction is easily seen in the Fourier path integral for the harmonic oscillator propagator, see e.g. ch. 1.2 in Ref. [3].

In the mathematical literature this is a well-known result: Nagano and Miyazaki [14] refer to several textbooks and cite an article by Hörmander from 1971 as earliest reference ⁵. In particular, their Proposition 2.5 (for the particular case $\xi = 0$)

$$\frac{1}{(2\pi)^{N/2}} \int d^N x \exp \left[\frac{i}{2} \sum_{j=1}^N x_j \mathcal{A}_{jk} x_k \right] = \frac{\exp \left(\frac{i\pi}{4} \text{sgn} \mathcal{A} \right)}{|\det \mathcal{A}|^{1/2}} \quad (4.4)$$

is the generalization of Eq. (3.2). Here

$$\text{sgn} \mathcal{A} = n_+ - n_- \quad (4.5)$$

denotes the *signature* (Ref. [25], p. 221) of the real, symmetric, non-singular matrix \mathcal{A} , i.e. the difference of positive and negative eigenvalues. Using $n_+ + n_- = N$ the phase factor in Eq. (4.4) thus is

$$\exp \left(\frac{i\pi}{4} N \right) \cdot \exp \left(-i\frac{\pi}{2} n_- \right). \quad (4.6)$$

While the first factor also shows up in the free propagator the second factor obviously describes the effect of negative eigenvalues, i. e. the Maslov phase.

³In particular in some quantum field theory texts where the harmonic oscillator serves as an example of exact path integration, e.g. in Refs. [18], [19], [20] or in the prepublication version of Ref. [21]. A detailed exposition of the Maslov correction is given in Ref. [22]. An early proof for this phenomenon was provided by Pechukas [23] who evaluated the time-evolution operator at time $\pi < \Omega T < 2\pi$ with the help of the composition law $\hat{U}(T, 0) = \hat{U}(T, T') \hat{U}(T', 0)$ with $0 < \Omega(T - T'), \Omega T' < \pi$ (see also Problem 9 in Ref. [3]).

⁴It is unclear to me how an analytic continuation from euclidean to real time will generate the Maslov phase. According to the Osterwalder-Schrader reconstruction theorem [24], extensively used in Quantum Field Theory for justifying Wick rotations, this should be possible.

⁵Thus calling the correction the "Maslov phase" seems to be not fully correct but only underlines the saying: *Most named effects in physics are not named after the first discoverer...*

4.1 The Maslov correction in the time-sliced path integral

I will be using the usual time-slicing method for evaluating the path integral in $d = 1$ dimensions (see, e.g. Ref.[3], section I.2) but with $N + 1$ intervals to simplify the notation. For accelerating the convergence of the discretized version to the continuum one, I will utilize the symmetric form of the Trotter product formula eq. (1.33)

$$\exp \left[-i\Delta T(\hat{T} + \hat{V}) \right] = \exp \left[-i\Delta T\hat{V}/2 \right] \cdot \exp \left[-i\Delta T\hat{T} \right] \cdot \exp \left[-i\Delta T\hat{V}/2 \right] + \mathcal{O}((\Delta T)^3), \quad (4.7)$$

applied to kinetic (\hat{T}) and potential (\hat{V}) energy operator. This is correct up to order $(\Delta T)^2$ where $\Delta T = (t_b - t_a)/(N + 1)$ is the time-step of the discretized version ⁶. This slightly modifies eq. (1.28) in that reference to

$$U(x_b, t_b; x_a, t_a) = \lim_{N \rightarrow \infty} \left(\frac{m}{2\pi i \Delta T} \right)^{(N+1)/2} \int_{-\infty}^{+\infty} dx_1 dx_2 \dots dx_N \cdot \exp \left\{ i\Delta T \sum_{j=1}^{N+1} \left[\frac{m}{2} \left(\frac{x_j - x_{j-1}}{\Delta T} \right)^2 - \frac{1}{2}V(x_j) - \frac{1}{2}V(x_{j-1}) \right] \right\} \quad (4.8)$$

where $x_0 = x_a$ and $x_{N+1} = x_b$ are fixed. Eq. (4.8) thus is based on an "exterior" average $\frac{V(x_j)+V(x_{j-1})}{2}$ for the potential whereas the usual "midpoint rule" with $V\left(\frac{x_j+x_{j-1}}{2}\right)$ is an "interior" average. In the continuum limit $\Delta T \rightarrow 0, N \rightarrow \infty$ there is, of course, no difference between these distinct discretization, but for finite ΔT there is. For simplicity, in the present note, I will use Eq. (4.8).

The prefactor $F(T)$ for the harmonic oscillator potential is thus obtained by putting $x_a = x_b = 0$ so that the classical action vanishes as well as terms with $V^{\text{h.o.}}(0) = 0$. For $N \geq 1$ this gives

$$F^{\text{h.o.}}(T) = U(0, T; 0, 0) = \lim_{N \rightarrow \infty} F_N^{\text{h.o.}}(T) \quad (4.9)$$

with

$$\begin{aligned} F_N^{\text{h.o.}}(T) &= \left(\frac{m}{2\pi i \Delta T} \right)^{\frac{N+1}{2}} \int_{-\infty}^{+\infty} dx_1 dx_2 \dots dx_N \exp \left\{ \frac{im}{2\Delta T} \left[x_N^2 + x_1^2 + \sum_{j=2}^N ((x_j - x_{j-1})^2 - (\Omega \Delta T)^2 \sum_{j=1}^N x_j^2) \right] \right\} \\ &= \left(\frac{m}{2\pi i \Delta T} \right)^{(N+1)/2} \int_{-\infty}^{+\infty} dx_1 dx_2 \dots dx_N \exp \left\{ \frac{im}{\Delta T} \left[\xi \sum_{j=1}^N x_j^2 - \sum_{j=2}^N x_j \cdot x_{j-1} \right] \right\} \end{aligned} \quad (4.10)$$

where I have defined

$$\xi := 1 - \frac{1}{2}(\Delta T)^2 \Omega^2 = 1 - \frac{1}{2} \frac{\Omega^2 T^2}{(N+1)^2} \quad (4.11)$$

and an empty sum is to be taken as zero.

Since these are all Gauss-Fresnel integrals they can be evaluated analytically also for finite N as demonstrated in Appendix A. Let us write the prefactor as in eq. (1.89) of Ref. [3]

$$F_N^{\text{h.o.}} =: \left(\frac{m}{2\pi i |f_N(\Omega T)|} \right)^{1/2} e^{i\Phi_N^{\text{Maslov}}(\Omega T)}. \quad (4.12)$$

Then one finds for finite N

$$\Omega f_N(\tau) = \frac{\tau}{N+1} U_N \left(1 - \frac{\tau^2}{4(N+1)^2} \right), \quad \Phi_N^{\text{Maslov}}(\tau) = -\frac{\pi}{2} \sum_{n=1}^N \Theta \left[\tau - 2(N+1) \sin \left(\frac{n\pi}{2(N+1)} \right) \right] \quad (4.13)$$

⁶Expressions which are correct to arbitrary high orders have been investigated in Refs. [26], [27] in terms of increasingly higher derivatives of the potential. In lattice field theories this amounts to constructing "improved actions", an example of these is given in Ref. [28].

where

$$\tau := \Omega T \quad (4.14)$$

is the dimensionless time and $U_N(z)$ the Chebyshev polynomial of the second kind. In Appendix A the continuum limit ($N \rightarrow \infty$, T fixed)

$$\Omega f_\infty(\tau) = \sin \tau, \quad \Phi_\infty^{\text{Maslov}}(\tau) = -\frac{\pi}{2} \sum_{n=1}^{\infty} \Theta(\tau - n\pi) \quad (4.15)$$

is also studied in detail.

4.2 Numerical implementation and results

The challenge is now to evaluate Eq. (4.10) with a finite number of time slices, i.e. a finite number N of intermediate integrals. To cope with the oscillating integrand I use N -dimensional spherical coordinates

$$\begin{aligned} x_1 &= R \cos(\phi_1) \\ x_2 &= R \sin(\phi_1) \cos(\phi_2) \\ x_3 &= R \sin(\phi_1) \sin(\phi_2) \cos(\phi_3) \\ &\vdots \\ x_{N-1} &= R \sin(\phi_1) \dots \sin(\phi_{N-2}) \cos(\phi_{N-1}) \\ x_N &= R \sin(\phi_1) \dots \sin(\phi_{N-2}) \sin(\phi_{N-1}) \end{aligned} \quad (4.16)$$

so that the most violent oscillations come from the infinite integral over the hyperradius as in the Gauss-Fresnel integral. Whereas $R \in [0, \infty]$, the integration over the angles ϕ_j is restricted:

$$\phi_1, \phi_2 \dots \phi_{N-2} \in [0, \pi] \quad \text{but} \quad \phi_{N-1} \in [0, 2\pi], \quad (4.17)$$

The volume element is

$$d^N x = R^{N-1} \sin^{N-2}(\phi_1) \sin^{N-3}(\phi_2) \dots \sin(\phi_{N-2}) dR d\phi_1 d\phi_2 \dots d\phi_{N-1} = R^{N-1} dR d\Omega_{N-1}. \quad (4.18)$$

Substituting $R = \sqrt{y\Delta T/m}$ Eq. (4.10) then reads

$$F_N^{\text{h.o.}}(\tau) = \sqrt{\frac{m}{8\pi i \Delta T}} (2\pi i)^{-N/2} \int d\Omega_{N-1} \int_0^\infty dy y^{N/2-1} \exp[i\omega_N(\phi_1 \dots \phi_{N-1}; \tau) y] \quad (4.19)$$

where

$$\omega_N(\phi_1 \dots \phi_{N-1}; \tau) = \left(\xi \sum_{j=1}^N x_j^2 - \sum_{j=2}^N x_j \cdot x_{j-1} \right) / R^2 = \xi - \sum_{j=2}^N x_j \cdot x_{j-1} / R^2. \quad (4.20)$$

By normalizing the prefactor to the free case trivial complex factors are eliminated. The free case is easily obtained by letting $\Omega \rightarrow 0$ in Eq. (4.13) so that $f_N \rightarrow T/(N+1)$, $\Phi_N^{\text{Maslov}} \rightarrow 0$. Thus

$$\begin{aligned} F_N^{\text{h.o.}}(\tau)/F_N^{\text{free}} &= \frac{1}{2} (2\pi i)^{-N/2} \int d\Omega_{N-1} \int_0^\infty dy y^{N/2-1} \exp[i\omega_N(\phi_1 \dots \phi_{N-1}; \tau) y] \\ &= \sqrt{\frac{\Delta T}{|f_N(\tau)|}} e^{i\Phi_N^{\text{Maslov}}(\tau)} \end{aligned} \quad (4.21)$$

directly gives magnitude and phase of the prefactor. Note that the phase is determined only modulo 2π , or *vice versa*

$$\phi_N^{\text{Maslov}} = \text{atan2}(\text{Re}F_N, \text{Im}F_N) + 2\pi n \quad , \quad n = 0, \pm 1, \pm 2 \dots \quad (4.22)$$

(see Eq. (A.33b)). We are free to "align", i. e. choose n in order to directly compare with the analytic result (4.15) without changing the physics.

The strategy to evaluate Eq. (4.21) numerically is the following: Perform the integration over the hyper-radius R by means of Ooura's integration formula for oscillatory integrals while the integration over the angles is done by standard integration routines. This is summarized in Table 1 which also lists the relevant accuracy parameters in these routines and their typical values.

routine/method	application/feature	Ref.	accuracy parameters	explanation	typical value
Ooura	double exponential for oscill. integrand deterministic	[13]	k_{max} : ϵ_{Ooura} :	summation cut-off in Eq. (2.1) smallest weight (Eq.(B.6))	50 – 80 10^{-8}
Double Exponential	general integrand deterministic	[7]	k_{max} : ϵ_{DE} :	as in Ooura smallest weight	50 10^{-8}
Gauss-Chebyshev (modified for complex integrand)	adaptive deterministic	[29]	m_{Cheby} : ϵ_{Cheby} :	max. # of function calls required rel. accuracy	511 10^{-3}
VEGAS	importance sampling Monte-Carlo	[30]	n_{call} : itm_x :	max. # of function calls max. # of iterations	$10^5 - 10^6$ 10

Table 1: Integration routines used (in order of appearance) with typical values of the corresponding accuracy parameters.

Let us start discussing the numerical results with the simplest (but already non-trivial) case $N = 1$, i.e. 2 time slices for the discretized path integral and thus no integral over an hyperspherical angle. Fig. 2 shows the numerical result when evaluating Eq. (4.19) for $N = 1$, i.e.

$$F_1^{\text{h.o.}}(\tau) = \sqrt{\frac{m}{2\Delta T}} \frac{S_0}{2\pi i} \int_0^\infty dy y^{-1/2} e^{i\omega_1 y} = \sqrt{\frac{m}{2\pi i \Delta T}} \frac{1}{\sqrt{\xi + i0^+}} \quad (4.23)$$

since $S_0 = 2$ (see Eq. (3.4)) and $\omega_1 \equiv \xi = 1 - \tau^2/8$ (see Eqs. (4.20), (4.11)). The extra Maslov phase of $-\pi/2$ acquired when passing the focal point at $\xi = 0$, i.e. $\tau \equiv \Omega T = \sqrt{8}$ is clearly seen ⁷ and very accurately reproduced by Ooura's integration routine.

⁷For better readability phases are plotted in degrees here and in the following figures.

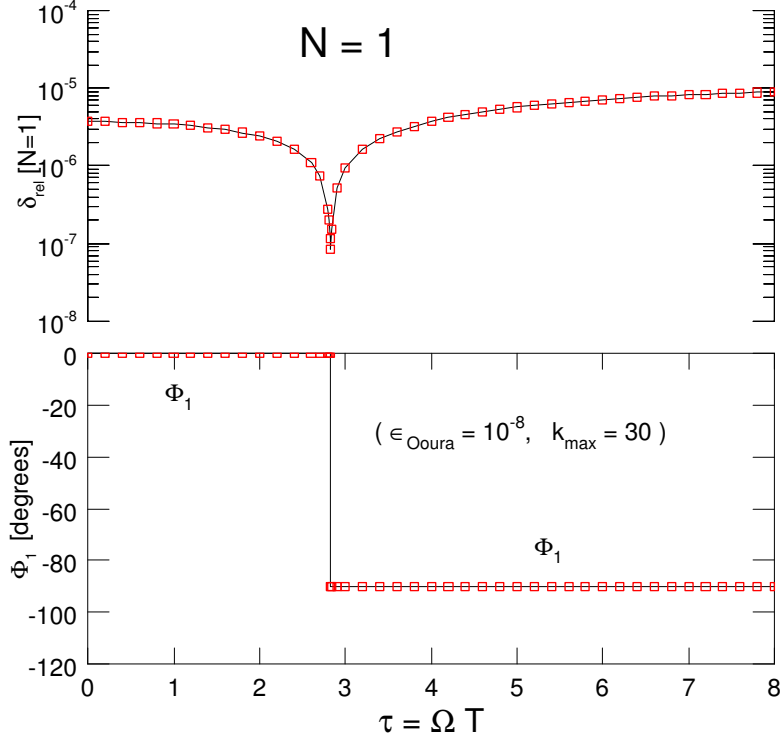


Fig. 2 : Upper panel: Relative complex deviation (as defined in Eq. (3.6)) of the numerical result for the prefactor of the harmonic oscillator propagator with $N = 1$ (i.e. 2 time slices in the path integral) from the exact ($N = 1$)-result. In the lower panel the resulting additional *Maslov* phase Φ_1 is plotted as a function of the dimensionless time $\tau = \Omega T$ where Ω denotes the oscillator frequency. The integral (4.21) was evaluated numerically with Ooura's formula (2.1) and is compared with the exact ($N = 1$)-result (black line) which has one focal point at $\tau = \sqrt{8} = 2.818\dots$

Unfortunately, this does not hold for $N = 2$ as Fig. 3 shows where the subsequent integration over the angle ϕ_1 is performed by the double exponential method: even by vastly increasing the number of function calls the relative complex deviation from the exact result

$$F_2^{\text{h.o.}}(\tau) = \sqrt{\frac{m}{8\pi i \Delta T}} \frac{1}{2\pi i} \int_0^{2\pi} d\phi_1 \int_0^\infty dy e^{i\omega_2(\phi_1)y} = \sqrt{\frac{m}{8\pi i \Delta T}} \frac{1}{2\pi} \int_0^{2\pi} d\phi_1 \frac{1}{\omega_2(\phi_1) + i0^+} \quad (4.24)$$

remains large ($O(1)$) near the two focal points. This may be due to the distribution

$$\frac{1}{\omega_2(\phi_1) + i0^+} = \frac{1}{\xi - \sin \phi_1 \cos \phi_1 + i0^+} = \mathcal{P} \frac{1}{\xi - \sin \phi_1 \cos \phi_1} - i\pi \delta(\xi - \sin \phi_1 \cos \phi_1) \quad (4.25)$$

which Ooura's routine tries to mimic by a $2k_{\text{max}} + 1$ finite number of terms but the subsequent double exponential integration rule cannot handle properly...

As an ad-hoc way out of this dilemma one may introduce an overall damping factor

$$\boxed{D_\eta(y) := e^{-\eta y}, \quad \eta > 0 \quad \text{"small"}} \quad (4.26)$$

into the y -integral. As shown in Fig. 4 this works for a damping factor $\eta = 0.001$ both for the standard double exponential integration routine as well as for a modified adaptive Gauss-Chebyshev integration method.

Indeed, from Eq. (4.19) it is seen that introducing the *ad hoc*-damping factor (4.26) amounts to replacing

$$\xi \longrightarrow \xi + i\eta \quad (4.27)$$

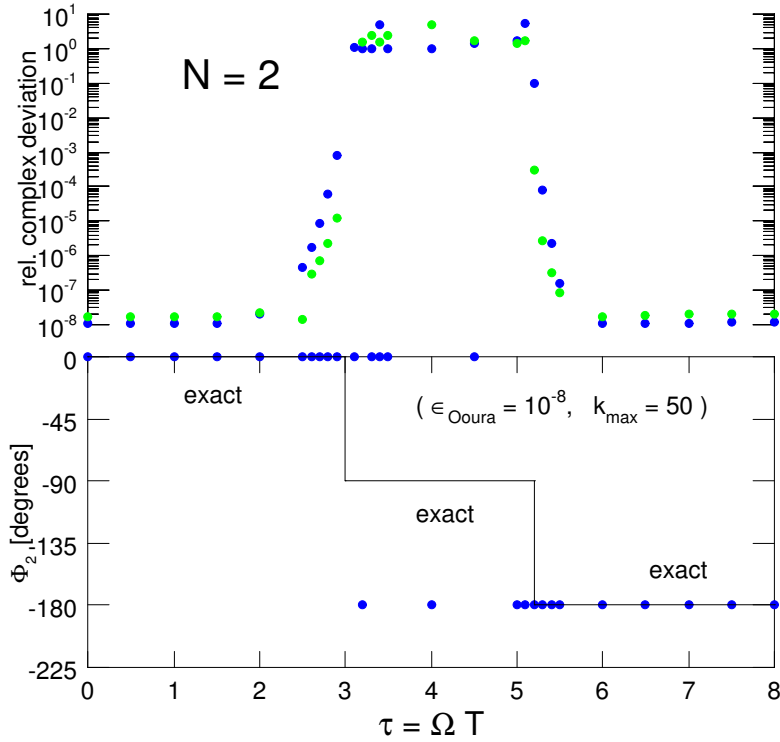


Fig. 3 : Prefactor of the harmonic oscillator propagator as function of the dimensionless time for the discretized version of the path integral with $N = 2$ (i.e. 3 time slices). The lower panel depicts the Maslov phase obtained when passing the two focal points (solid line: exact, points: numerical result). The upper panel shows the relative complex deviation of the numerical result from the exact one. The integration over the hyperradius has been performed with Ooura’s rule (with standard accuracy parameters) whereas the integration over the (only) one angle was done with the original double exponential (DE) rule of Ref. [7] choosing the same ϵ -parameter as for the oscillatory integral. Blue or green points have been obtained with $k_{\max}^{\text{DE}} = 50$ or 500.

or equivalently to shifting the focal points slightly into the complex plane. Then Eq. (4.25) changes into

$$\frac{1}{\omega_2(\phi_1) + i0^+} \longrightarrow \frac{1}{\omega_2(\phi_1) + i\eta} = \frac{\omega_2(\phi_1)}{\omega_2^2(\phi_1) + \eta^2} - i \frac{\eta}{\omega_2^2(\phi_1) + \eta^2} \quad (4.28)$$

which is finite and a well-known representation of these distributions for $\eta \rightarrow 0$. The exact value of the harmonic oscillator prefactor with damping is worked out in Appendix A, Eqs. (A.32), (A.34).

As shown in Fig. 5 the adaptive integration routine [29] (slightly modified to allow complex integrands and relative complex error to be achieved) and the classic VEGAS program [30] (applied to real and imaginary parts separately) give nearly identical results when the same number of function calls is used. The adaptive routine does a little bit better away from the focal points but not in their vicinity. The advantage of the Monte-Carlo evaluation is that it also provides error estimates for the real and imaginary part of the integral which – by error propagation – allow an estimate of the error in phase and magnitude of the path integral prefactor. However, due to the delicate integrand these estimates typically are too small by a factor of two and more.

Table 2 displays the numerical results for the ($N = 3$)-Gauss-Chebyshev results depicted in Fig. 5. The complex harmonic oscillator prefactor starts in the 4th quadrant and moves clockwise with increasing time. After passing through 3 focal points the accumulated Maslov phase is $< -\pi$. The numerical result then enters the second quadrant which may be interpreted as a positive phase. Choosing $n = -1$ in Eq. (4.22) ”aligns” it with the analytic result and allows a meaningful comparison. As a well-defined Fresnel integral the numerical result for the prefactor – as given in the second column of Table 2 – is, of course, unambiguous and does not depend on the chosen branch of a multi-valued function as discussed in Ref. [31].

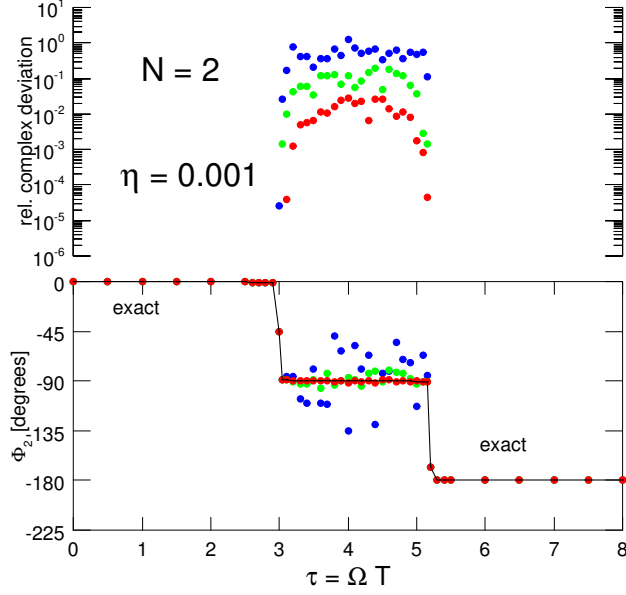


Fig. 4 : Same as in Fig. 3 but now with an additional damping $\exp(-\eta y)$ and $\eta = 0.001$. An adaptive Gauss-Chebyshev rule [29] was used for integration over the only one angle with the maximal number of function calls $m_{\text{Cheby}} = 1023$ (blue points), 4095 (green points), 8191 (red points).

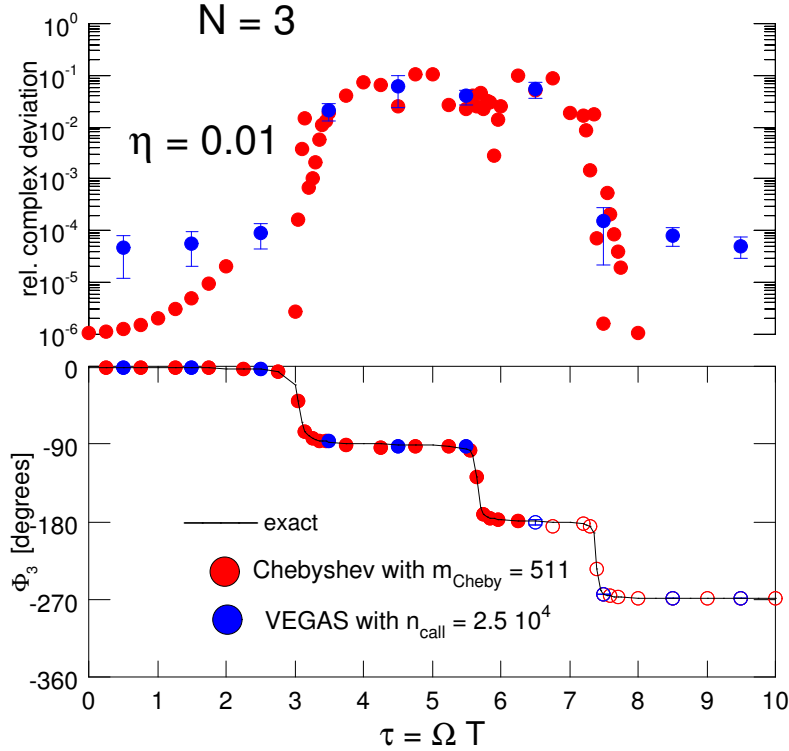


Fig. 5 : Same as in Fig. 4 but for $N = 3$ and damping $\eta = 0.01$. Results with the adaptive Gauss-Chebyshev rule for integration over the the two angles angles (maximal number of function calls $m_{\text{Cheby}} = 511$, required relative accuracy 10^{-5}) are compared with the ones from the Monte-Carlo routine VEGAS with $n_{\text{call}} = 2.5 \cdot 10^4$ function calls. Open circles indicate values where the $n = -1$ alignment (4.22) has been applied.

τ	$F_3^{\text{h.o.}}/F_3^{\text{free}}$	$\delta_{\text{rel}}[F_3^{\text{h.o.}}]$	Φ_3^{Maslov} [degrees]
0.0	+0.999 - 0.025 i	$1.05 \cdot 10^{-6}$	($n = 0$) - 1.4
0.5	+1.019 - 0.026 i	$1.22 \cdot 10^{-6}$	- 1.5
1.0	+1.084 - 0.029 i	$2.01 \cdot 10^{-6}$	- 1.6
1.5	+1.214 - 0.037 i	$4.90 \cdot 10^{-6}$	- 1.8
2.0	+1.464 - 0.057 i	$2.03 \cdot 10^{-5}$	- 2.2
2.5	+2.043 - 0.124 i	$5.98 \cdot 10^{-14}$	- 3.5
3.0	+5.266 - 2.014 i	$2.74 \cdot 10^{-6}$	-20.9
3.5	+0.079 - 2.563 i	$1.87 \cdot 10^{-2}$	-88.2
4.0	+0.094 - 2.128 i	$7.47 \cdot 10^{-2}$	-87.5
4.5	+0.040 - 1.917 i	$2.51 \cdot 10^{-2}$	-88.8
5.0	+0.047 - 2.029 i	$1.04 \cdot 10^{-1}$	-88.7
5.5	-0.475 - 4.235 i	$2.25 \cdot 10^{-2}$	-96.4
6.0	-2.797 - 0.085 i	$2.54 \cdot 10^{-2}$	-178.2
6.5	-2.016 - 0.113 i	$5.18 \cdot 10^{-2}$	-176.8
7.0	-2.038 + 0.020 i	$1.94 \cdot 10^{-2}$	+179.4 $\xrightarrow{n=-1}$ -180.6
7.5	-0.316 + 2.935 i	$1.59 \cdot 10^{-11}$	+96.2 \rightarrow -263.8
8.0	-0.025 + 0.999 i	$1.05 \cdot 10^{-6}$	+91.4 \rightarrow -268.6
8.5	-0.009 + 0.606 i	$1.62 \cdot 10^{-8}$	+90.9 \rightarrow -269.1
9.0	-0.005 + 0.421 i	$7.55 \cdot 10^{-10}$	+90.7 \rightarrow -269.3
9.5	-0.003 + 0.312 i	$6.53 \cdot 10^{-11}$	+90.5 \rightarrow -269.5
10.0	-0.002 + 0.242 i	$8.54 \cdot 10^{-12}$	+90.4 \rightarrow -269.6

Table 2: The (complex) harmonic oscillator prefactor (normalized to the free case) for $N = 3$ obtained numerically with Ooura’s and Gauss-Chebyshev integration routines (damping $\eta = 0.01$) as function of the dimensionless time $\tau = \Omega T$. With no damping the focal points occur at $\tau = 3.061, 5.656, 7.391$ (see Eq. (A.12)) where nearly step-like changes of the phase can be seen in Fig. 5). The third column gives the relative complex deviation of the numerical result from the exact value. In the last column the calculated Maslov phase is listed together with the ”alignment” (addition of $2\pi n$, $n = -1$, see Eq. (4.22)) when the prefactor enters the second quadrant in the complex plane at $\tau \simeq 7$.

For larger values of N deterministic integration routines become inefficient (the infamous ”curse of dimensions”) so that only stochastic methods remain. Figs. 6 and 7 demonstrate that the VEGAS Monte-Carlo method still works for $N = 5$ and $N = 8$ although larger values of the damping parameter η are required to get stable results. Longer Monte-Carlo runs (one data point with 10^6 function calls in Fig. 7 took about 25 minutes on a standard 2.5 GHz PC) are also feasible to improve the statistics.

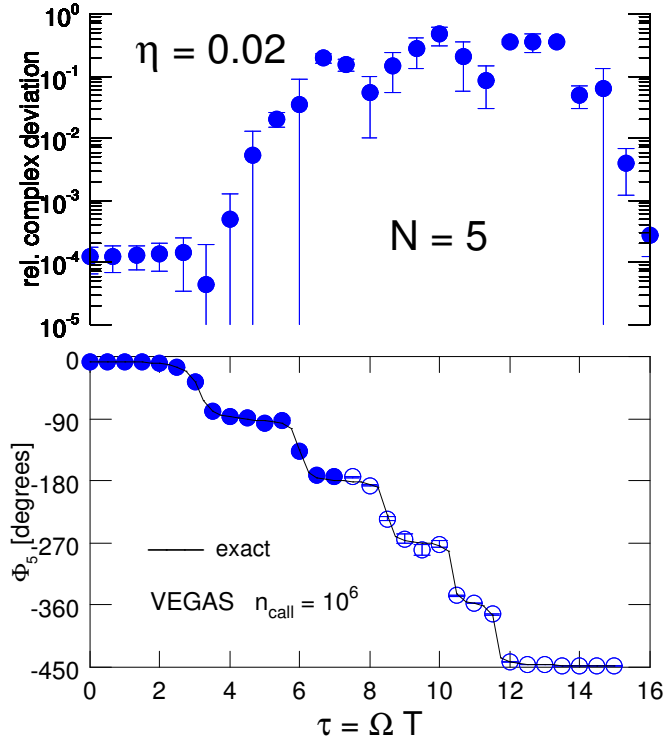


Fig. 6 : Same as in Fig. 5 but for $N = 5$ and $\eta = 0.02$.

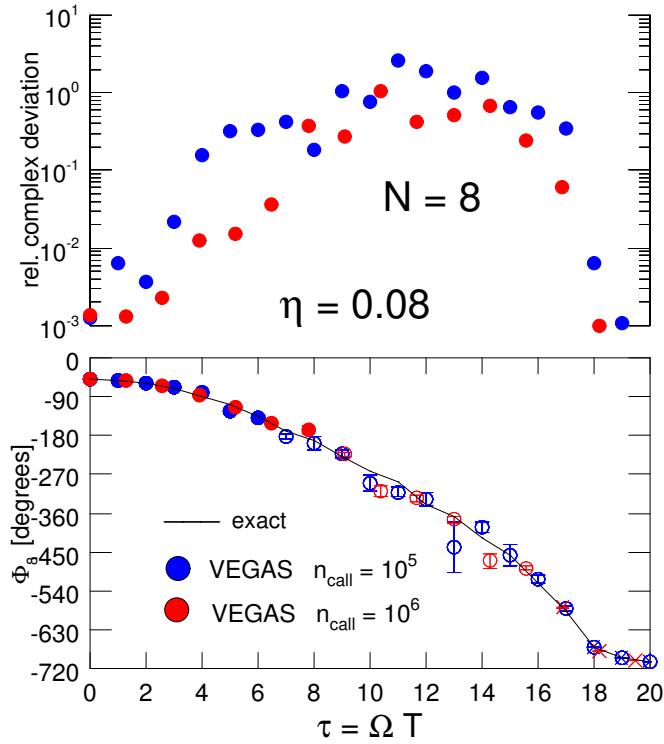


Fig. 7 : Same as in Fig. 5 but for $N = 8$ and $\eta = 0.08$. For the last 3 data points (indicated by crosses) an alignment (4.22) with $n = -2$ was applied.

5. Summary and Outlook

Real-time path integrals for dynamic quantum processes are a numerical challenge as one has to steer between conflicting requirements: on the one hand the time-step ΔT has to be small to reach the continuum limit while the dimension N of the integrals has to be large enough to capture the relevant time scale $T = (N + 1)\Delta T$. While this can be handled in imaginary time and is widely used to obtain information on static properties time-dependent processes like scattering require (functional) integration over rapidly oscillating functions.

As prototype for these challenges I have evaluated numerically Gauss-Fresnel oscillatory integrals of dimension up to $N = 20$, i.e. basically the free particle propagator. The key to a successful achievement was Oura's double exponential integration method [13] combined with the use of hyperspherical co-ordinates to isolate the most rapidly oscillating degree of freedom.

In a second application these tools allowed to calculate numerically the prefactor in the harmonic oscillator propagator and thereby the Maslov phase which emerges each time when the quantum particle passes through a (singular) focal point. In the discretized version of the path integral the number of focal points equals the dimension of the oscillatory integral over hyperradius and angles which in the present work went up to $N = 8$.

Unfortunately these singularities required an additional small damping factor in order to obtain stable results. Nevertheless this may be considered as an encouraging step to evaluate real-time path integrals directly e.g for scattering in a finite-range potential [32], [33]. This is due to several reasons: First, the unwanted damping may be dealt with by an extrapolation of the results to zero damping similar to the extrapolation to small quark (or pion) mass in lattice gauge theories [34]. In addition, one may expect that "caustic" singularities will be avoided or alleviated in exact path integral formulations for the T -matrix which go beyond the semiclassical approximation. Also the peculiar properties of the harmonic potential will be absent in short-range interactions.

While it seems that $N = 8$ is a far cry from the true continuum limit ($N \rightarrow \infty$) of functional integrals improved effective actions [26] may allow larger time steps and thus fewer time slices. Whether this leads to a reliable numerical evaluation of functional integrals for scattering requires further investigation.

Acknowledgement: I would like to thank Matthias who enabled me to perform the numerical calculations on my home computer and Michael Spira for supplying me with his version of the VEGAS program and for the hospitality in the PSI Particle Theory Group.

Appendix

A. Maslov phase in the discretized path integral

Here I give the results for the prefactor in the discretized path integral for the harmonic oscillator, first for a few low-dimensional cases and then for an arbitrary number of time slices. This then allows to study the continuum limit.

$N = 1$:

$$F_1^{\text{h.o.}}(T) = \frac{m}{2\pi i \Delta T} \int_{-\infty}^{+\infty} dx_1 \exp \left\{ \frac{im}{2\Delta T} (2 - (\Delta T)^2 \Omega^2) x_1^2 \right\} = \left(\frac{m}{2\pi i \Delta T} \right)^{1/2} \frac{1}{\sqrt{2\xi}} \quad (\text{A.1})$$

where ξ has been defined in Eq. (4.11). It is seen that in this rough approximation for the path integral (just 2 time slices!) a focal point occurs at $\xi_1 = 0$ where the argument of the inverse square root turns negative. Using $\Delta T = T/2$ this translates into

$$\Omega T = \sqrt{8} = 2.828\dots =: X_1^{(1)} \quad (\text{A.2})$$

compared to the exact continuum value of $\pi = 3.141\dots$. Thus

$$\Omega f_1(\tau) = \tau \left(1 - \frac{\tau^2}{8} \right), \quad \Phi_1^{\text{Maslov}}(\tau) = -\frac{\pi}{2} \Theta \left(\tau - X_1^{(1)} \right). \quad (\text{A.3})$$

$N = 2$:

$$\begin{aligned} F_2^{\text{h.o.}}(T) &= \left(\frac{m}{2\pi i \Delta T} \right)^{3/2} \int_{-\infty}^{+\infty} dx_1 dx_2 \exp \left\{ \frac{im}{2\Delta T} \left[x_1^2 + x_2^2 + (x_2 - x_1)^2 - \Omega^2 (\Delta T)^2 (x_1^2 + x_2^2) \right] \right\} \\ &= \left(\frac{m}{2\pi i \Delta T} \right)^{3/2} \int_{-\infty}^{+\infty} dx_1 dx_2 \exp \left\{ \frac{im}{\Delta T} \left[\xi \left(\underbrace{x_1 - x_2/2\xi}_{=: x'_1} \right)^2 + \left(\xi - \frac{1}{4\xi} \right) x_2^2 \right] \right\}. \end{aligned} \quad (\text{A.4})$$

After shifting the integration variable $x_1 \rightarrow x'_1$ one obtains

$$F_2^{\text{h.o.}}(T) = \left(\frac{m}{2\pi i \Delta T} \right)^{1/2} \frac{1}{\sqrt{\xi}} \frac{1}{\sqrt{4\xi - 1/\xi}}. \quad (\text{A.5})$$

With $\Delta T = T/3$ one sees that in this approximation there are 2 focal points during the evolution of the harmonically bound particle: with increasing time one at

$$\xi_1 = \frac{1}{2} \implies \Omega T = 3 =: X_1^{(2)} \quad (\text{A.6})$$

(instead of the exact value π) and another one at

$$\xi_2 = -\frac{1}{2} \implies \Omega T = 3\sqrt{3} = 5.196\dots =: X_3^{(2)} \quad (\text{A.7})$$

(instead of the exact value $2\pi = 6.283\dots$). Note that

$$\xi = 0 \implies \Omega T = 3\sqrt{2} = 4.242\dots =: X_2^{(2)} \quad (\text{A.8})$$

is *not* a focal point as the prefactor does not diverge here.

Thus from Eq. (A.5) one has

$$\Omega f_2(\tau) = \tau \left(1 - \frac{\tau^2}{9}\right) \left(1 - \frac{\tau^2}{27}\right). \quad (\text{A.9})$$

Obviously the function $4\xi - 1/\xi$ is negative for $0 < \xi < 1/2$ and for $\xi < -1/2$. With $\xi = 1 - \tau^2/18$ the ($N = 2$)-approximation to the path integral thus gives the following Maslov phase

$$\begin{aligned} \Phi_2^{\text{Maslov}}(\tau) &= -\frac{\pi}{2} \left[\Theta\left(\tau - X_1^{(2)}\right) \Theta\left(X_2^{(2)} - \tau\right) + \Theta\left(\tau - X_2^{(2)}\right) + \Theta\left(\tau - 3\sqrt{3}\right) \right] \\ &= -\frac{\pi}{2} \sum_{n=1, n \neq 2}^3 \Theta\left(\tau - X_n^{(2)}\right) \end{aligned} \quad (\text{A.10})$$

as function of $\tau = \Omega T$. Note that naively combining the square roots in Eq. (A.5) into $(4\xi^2 - 1)^{-1/2}$ (without considering their phases in the complex plane) would give the wrong result that the Maslov phase Φ_2 would vanish for $\xi < -1/2$, i.e. $\tau > 3\sqrt{3}$. Note also that in the final result (A.10) the point $\tau = X_2^{(2)}$ does not appear: only the true focal points *add* a phase $-\pi/2$ when the particle passes through it during its time evolution.

$N = 3$:

$$\begin{aligned} F_3^{\text{h.o.}}(T) &= \left(\frac{m}{2\pi i \Delta T}\right)^2 \int_{-\infty}^{+\infty} dx_1 dx_2 dx_3 \exp \left\{ \frac{im}{2\Delta T} \left[x_1^2 + x_3^2 + (x_2 - x_1)^2 + (x_3 - x_2)^2 - (\Omega \Delta T)^2 (x_1^2 + x_2^2 + x_3^2) \right] \right\} \\ &= \left(\frac{m}{2\pi i \Delta T}\right)^2 \int_{-\infty}^{+\infty} dx_1 dx_2 dx_3 \exp \left\{ \frac{im}{2\Delta T} \left[2\xi \left(\underbrace{x_1 - x_2/2\xi}_{=x'_1} \right)^2 + \left(2\xi - \frac{1}{\xi} \right) x_2^2 + 2\xi \left(\underbrace{x_3 - x_2/2\xi}_{=: x'_3} \right)^2 \right] \right\} \\ &= \left(\frac{m}{2\pi i \Delta T}\right)^{1/2} \frac{1}{\sqrt{2\xi}} \frac{1}{\sqrt{2\xi - 1/\xi}} \frac{1}{\sqrt{2\xi}}. \end{aligned} \quad (\text{A.11})$$

With $\Delta T = T/4$ one finds that there are 3 focal points at

$$\begin{aligned} \xi_1 = \frac{1}{\sqrt{2}} &\implies \Omega T = 4\sqrt{2 - \sqrt{2}} = 3.0614\dots =: X_1^{(3)} \\ \xi_2 = 0 &\implies \Omega T = 4\sqrt{2} = 5.6556\dots =: X_2^{(3)} \quad (\text{here a genuine focal point with multiplicity 2}) \\ \xi_3 = -\frac{1}{\sqrt{2}} &\implies \Omega T = 4\sqrt{2 + \sqrt{2}} = 7.3910\dots =: X_3^{(3)} \end{aligned} \quad (\text{A.12})$$

instead of $\Omega T = n\pi, n = 1, 2, 3 \dots$ and therefore

$$\Omega f_3(\tau) = \tau \left(1 - \frac{\tau^2}{32}\right) \left(1 - \frac{\tau^2}{8} + \frac{\tau^4}{512}\right) \quad (\text{A.13})$$

$$\begin{aligned} \Phi_3^{\text{Maslov}}(\tau) &= -\frac{\pi}{2} \left[\Theta\left(\tau - X_1^{(3)}\right) \Theta\left(X_2^{(3)} - \tau\right) + 2\Theta\left(\tau - X_2^{(3)}\right) + \Theta\left(\tau - X_3^{(3)}\right) \right] \\ &= -\frac{\pi}{2} \sum_{n=1}^3 \Theta\left(\tau - X_n^{(3)}\right) \end{aligned} \quad (\text{A.14})$$

N arbitrary:

The standard method to calculate the prefactor for quadratic Lagrangians in the continuum limit is the Gel'fand-Yaglom method (see, e.g. Ref. [17], ch. 6 or Ref. [3] ch. 1.3) which leads to a differential equation for $f(T)$. The same method can also be used to evaluate $f_N(\tau)$ for finite ΔT by a recurrence relation: Define $p_0(\xi) = 1, p_1(\xi) = 2\xi$ and calculate

$$p_{j+1}(\xi) = 2\xi p_j(\xi) - p_{j-1}(\xi), \quad j = 1, 2 \dots N-1. \quad (\text{A.15})$$

Then

$$\Omega f_N(\tau) = \frac{\tau}{N+1} p_N \left(\xi = 1 - \frac{\tau^2}{2(N+1)^2} \right). \quad (\text{A.16})$$

This recurrence relation may be solved either by standard methods (see, e.g. Ref. [35]) or by examination of the recurrence relations for the classical orthogonal polynomials⁸. Although both $T_N(\xi)$ and $U_N(\xi)$ obey the same recurrence relation, only the Chebyshev polynomials of the second kind fulfill the initial condition $p_1(\xi) = 2\xi$ and therefore the final result is

$$p_N(\xi) = U_N(\xi) \implies \Omega f_N(\tau) = \frac{\tau}{N+1} U_N \left(1 - \frac{\tau^2}{2(N+1)^2} \right). \quad (\text{A.17})$$

With $U_0(\xi) = 1$, $U_1(\xi) = 2\xi$, $U_2(\xi) = 4\xi^2 - 1$, $U_3(\xi) = 8\xi^3 - 4\xi$ (Ref. [37] eq. 8.943) the explicit results obtained above are reproduced. Since (Ref. [36], eq. 22.3.16)

$$U_N(\xi) = \frac{\sin((N+1)\arccos\xi)}{\sin(\arccos\xi)} \quad (\text{A.18})$$

the zeroes of this function are real and given by the simple expression (Ref. [36], eq. 22.16.5)

$$\xi_n^{(N)} = \cos\left(\frac{n}{N+1}\pi\right) \quad n = 1, 2, \dots, N. \quad (\text{A.19})$$

Using the definition (4.11) this translates into the following formula for the (positive) time to reach the n^{th} focal point

$$\Omega T_n \equiv X_n^{(N)} = 2(N+1) \sin\left(\frac{n}{2(N+1)}\pi\right) \quad (\text{A.20})$$

in which the correct continuum limit $N \rightarrow \infty$ is evident. Since the Chebyshev polynomial of the second kind $U_N(\xi)$ is a polynomial of order N with real zeros $\xi_n^{(N)}$ it may be written as

$$U_N(\xi) = C_N \prod_{n=1}^N (\xi - \xi_n^{(N)}) \quad (\text{A.21})$$

where the normalization factor $C_N = 2^N$ is a consequence of the recurrence relation (A.15) which just gives this factor for the leading power of ξ (alternatively one can employ the explicit expression Eq. 22.3.7 in Ref. [36]). Upon taking the inverse square root of $p_N(\xi)$ for the prefactor (see Eqs. (4.12, A.16)) each factor contributes a phase of $-\pi/2$ whenever it becomes negative, i.e. $\xi < \xi_n^{(N)}$. Thus

$$\Phi_N^{\text{Maslov}}(\xi) = -\frac{\pi}{2} \sum_{n=1}^N \Theta(\xi_n^{(N)} - \xi), \quad (\text{A.22})$$

a discontinuous function of the time.

The continuum limit for the function $f_N(\tau)$ in Eq. (A.17) is more involved but may be derived by expressing it as a hypergeometric function

$$\Omega f_N(\tau) = \tau \cdot {}_2F_1(a, b; c; z) = \tau \cdot \sum_{n=0}^{\infty} \frac{(a)_n (b)_n}{(c)_n} \frac{z^n}{n!} \quad (\text{A.23})$$

with

$$a = -N, \quad b = N+2, \quad c = \frac{3}{2}, \quad z = \frac{\tau^2}{4(N+1)^2} \quad (\text{A.24})$$

⁸See, e.g. Ref. [36], eq. 22.7.4 for the Chebyshev polynomials of the first kind $T_N(\xi)$ and eq. 22.7.5 for the ones of the second kind $U_N(\xi)$.

by means of eq. 22.5.48 in Ref. [36]. Thus

$$\Omega f_N(\tau) =: \sum_{n=0}^N d_n \tau^{2n+1} = \tau - \frac{N^2 + 2N}{(N+1)^2} \frac{\tau^3}{6} + \frac{(N-1)N(N+2)(N+3)}{(N+1)^4} \frac{\tau^5}{120} + \dots \quad (\text{A.25})$$

The first three expansion coefficients agree with the explicit calculations for $N = 1, 2, 3$ and tend to the first three coefficients in the series expansion of $\sin \tau$. From the series expansion of the hypergeometric function one deduces that the n^{th} term reads

$$d_n = \frac{(-N)_n (N+2)_n}{(3/2)_n} \frac{1}{n!} \left[\frac{1}{4(N+1)^2} \right]^n. \quad (\text{A.26})$$

This can be evaluated by expressing the Pochhammer symbols as factorials

$$(-N)_n = (-)^n \frac{N!}{(N-n)!}, \quad (N+2)_n = \frac{(N+n+1)!}{(N+1)!}, \quad \left(\frac{3}{2}\right)_n = \frac{(2n+1)!}{2^{2n} n!} \quad (\text{A.27})$$

and gives

$$d_n = \frac{(-)^n}{(2n+1)!} \prod_{k=1}^{2n+1} \left(\frac{N-n+k}{N+1} \right) \xrightarrow{N \rightarrow \infty, n \text{ fixed}} \frac{(-)^n}{(2n+1)!} \implies \Omega f_N(\tau) \xrightarrow{N \rightarrow \infty} \sin \tau. \quad (\text{A.28})$$

with damping:

If the damping factor (4.26) is used to regulate the discrete path integral the variable ξ is replaced by

$$\xi \longrightarrow \bar{\xi} := \xi + i\eta \quad (\text{A.29})$$

which leads to the following modifications: Knowing that $p_N(\xi)$ is a polynomial of degree N with zeroes at $\xi_n^{(N)}$ (see Eq. (A.19)) one can immediately write

$$p_N(\bar{\xi}) = 2^N \prod_{n=1}^N \left(\bar{\xi} - \xi_n^{(N)} \right) = 2^N \prod_{n=1}^N \left(\xi - \xi_n^{(N)} + i\eta \right) \quad (\text{A.30})$$

As before this product formula can now be used to calculate the prefactor of the damped harmonic oscillator path integral with each factor contributing separately to the inverse (principal value) square root

$$F_N^{(\text{damped h.o.})}(T; \eta) = \left(\frac{m}{2\pi i \Delta T} \right)^{1/2} 2^{-N/2} \prod_{n=1}^N \left[\xi - \xi_n^{(N)} + i\eta \right]^{-1/2}, \quad \xi = 1 - \frac{1}{2} \left(\frac{\Omega T}{N+1} \right)^2. \quad (\text{A.31})$$

From this one can read off the exact Maslov phase as

$$\Phi_N^{\text{Maslov, damped}}(\tau; \eta) = -\frac{1}{2} \sum_{n=1}^N \arg \left(\xi - \xi_n^{(N)} + i\eta \right) \quad (\text{A.32})$$

with the standard definitions for the argument of a complex quantity

$$\arg(z = x + iy) = \arctan \frac{y}{x} + \pi \Theta(-x) \operatorname{sgn} y, \quad -\pi < \arg z \leq \pi, \quad -\frac{\pi}{2} \leq \arctan \frac{y}{x} \leq \frac{\pi}{2} \quad (\text{A.33a})$$

$$\equiv \operatorname{atan2}(y, x) \quad (\text{A.33b})$$

Note that the phase is now a continuous function of ξ , i.e. of time $\tau = \Omega T$. The modulus of the prefactor is

$$\left| F_N^{(\text{damped h.o.})}(\xi; \eta) \right| = \left(\frac{m}{2\pi \Delta T} \right)^{1/2} 2^{-N/2} \prod_{n=1}^N \left[\left(\xi - \xi_n^{(N)} \right)^2 + \eta^2 \right]^{-1/4}. \quad (\text{A.34})$$

B. Some numerical details: Step size and accuracy

Inevitably the sum over k in Eq. (2.1) has to be restricted to a finite number of terms: $|k| \leq k_{\max}$. Then we need to know which step size h one has to take to get results accurate up to a given precision. This can be determined by examining the asymptotic behaviour of $\phi(t = kh)$. Let us write

$$\phi(t) = t + t \frac{e^{-a(t)}}{1 - e^{-a(t)}} = t + t \frac{1}{e^{a(t)} - 1} \quad \text{with} \quad a(t) := 2t + \alpha(1 - e^{-t}) + \beta(e^t - 1) \quad (\text{B.1})$$

and consider first the limit $t \rightarrow +\infty$. Obviously

$$a(t) \xrightarrow{t \rightarrow +\infty} \beta e^t + 2t + \alpha - \beta + \mathcal{O}(e^{-t}) \quad (\text{B.2})$$

grows exponentially and the factor in the curly brackets in Eq. (2.1) becomes

$$\left\{ \exp \left[i \operatorname{sgn}(\omega) \frac{\pi}{h} \phi(kh) \right] - (-1)^k \right\} = (-1)^k \left\{ \exp \left[i \operatorname{sgn}(\omega) \frac{k\pi}{e^{a(kh)} - 1} \right] - 1 \right\} \\ \xrightarrow{kh \rightarrow +\infty} (-1)^k \left\{ i \operatorname{sgn}(\omega) k\pi e^{-a(kh)} + \mathcal{O}(e^{-2a(kh)}) \right\} \quad (\text{B.3})$$

leading to a double exponential decay of terms with $k \simeq k_{\max}$ as desired

Requiring a suppression to size ϵ_{Ooura} we demand (cf. eq. (5. 19) in Ref. [11])

$$\exp[-\beta e^{k_{\max} h}] \leq \epsilon_{\text{Ooura}} \implies h \geq \frac{1}{k_{\max}} \ln \left(-\frac{1}{\beta} \ln \epsilon_{\text{Ooura}} \right). \quad (\text{B.4})$$

Since the step size h should be as small as possible this translates into an equality, i.e. a determination of the step size once the maximal number $2k_{\max} + 1$ of function calls and the accuracy parameter ϵ_{Ooura} are chosen. For large negative values of $t = kh$ one finds

$$\phi(t) \xrightarrow{t \rightarrow -\infty} -\exp \left(-\alpha e^{|t|} + 2t + \mathcal{O}(\ln |t|) \right) \implies \phi'(t) \rightarrow -\alpha \exp \left(-\alpha e^{|t|} + \mathcal{O}(t, \ln |t|) \right). \quad (\text{B.5})$$

Since $\phi'(kh)$ is the weight in Ooura's integration rule the terms with $k \simeq -k_{\max}$ will be suppressed double exponentially if

$$\exp[-\alpha e^{k_{\max} h}] \leq \epsilon_{\text{Ooura}} \implies h \geq \frac{1}{k_{\max}} \ln \left(-\frac{1}{\alpha} \ln \epsilon_{\text{Ooura}} \right). \quad (\text{B.6})$$

As $\alpha < \beta$ this is a stronger requirement than the one in Eq. (B.4). Note that Eq. (B.6) is an implicit equation for the step size as $\alpha = \alpha(h)$ (see Eq. (2.3)). We solve it by a few iterations starting with $\alpha_{(0)} = \beta$.

Calculations in this work have been performed in double-precision arithmetic. Nevertheless the numerical implementation require some care when evaluating small terms as "smallness by subtraction" leads to a loss of accuracy. Here this is exacerbated by the fact that these terms are weighted by a (large) power of the hyperradius which peaks at $k \simeq k_{\max}$ although finally made small by the double exponential decay. One could use a power series expansion as indicated in the last line of Eq. (B.3) but a simpler remedy is not to evaluate directly $\exp(ix) - 1$ for small x but instead $\exp(ix) - 1 = 2i \sin(x/2) \exp(ix/2)$, i.e. making them "small by multiplication".

References

- [1] R. P. Feynman and A. R. Hibbs: *Quantum Mechanics and Path Integrals*, emended by D. F. Styer, Dover, Mineola (2010).
- [2] H. Kleinert: *Path Integrals in Quantum Mechanics, Statistics, Polymer Physics, and Financial Markets*, 3rd Edition, World Scientific, New Jersey (2004).
- [3] R. Rosenfelder: "Path Integrals in Quantum Physics", arXiv: 1209.1315v4 [nucl-th]
- [4] <https://indico.mpp.mpg.de/event/6610/contributions/19082/attachments/13514/15146/hahn.pdf>
- [5] Ph. J. Davis and Ph. Rabinowitz: *Methods of Numerical Integration*, Academic Press, New York (1984)
- [6] R. Lambert and N. Makri: "Quantum-classical path integral. I. Classical memory and weak quantum nonlocality", *J. Chem. Phys.* **137** (2012) 22A552.
- [7] H. Takahashi and M. Mori: "Double exponential formulas for numerical integration", *Publ. RIMS, Kyoto Univ.* **9** (1974), 721 – 741.
- [8] M. Mori: "Discovery of the double exponential transformation and its developments", *Publ. RIMS, Kyoto Univ.* **41** (2005), 897 — 935.
- [9] D. H. Bailey, J. M. Borwein, D. Broadhurst and W. Zudilin: "Experimental Mathematics and Mathematical Physics", arXiv:1005.0414.
- [10] T. Ooura and M. Mori: "The double exponential formula for oscillatory functions over the half infinite interval", *J. Comp. Appl. Math.* **38** (1991), 353 – 360.
- [11] R. Rosenfelder: "On the numerical evaluation of a class of oscillatory integrals in worldline variational calculations", arXiv: hep-ph/0603161v3.
- [12] T. Ooura and M. Mori: "A robust double exponential formula for Fourier-type integrals", *J. Comp. Appl. Math.* **112** (1999), 229 – 241.
- [13] T. Ooura: "A Double Exponential Formula for the Fourier Transform", *Publ. RIMS, Kyoto Univ.* **41** (2005), 971 – 977.
- [14] T. Nagano and N. Miyazaki: "On singular points and oscillatory integrals", arXiv:1906.01438.
- [15] T. Nagano and N. Miyazaki: "General Fresnel integrals as oscillatory integrals with positive real power phase functions and applications to asymptotic expansions", arXiv:2005.12754.
- [16] V. P. Maslov and M. V. Fedoriuk: *Semi-classical Approximations in Quantum-Mechanics*, Reidel, Dordrecht (1981).
- [17] L. S. Schulman: *Techniques and Applications of Path Integration*, J. Wiley, New York (1981).
- [18] A. Das: *Field Theory. A Path Integral Approach*, World Scientific Lecture Notes in Physics - Vol. 75, Second Edition, World Scientific, Singapore (2012).
- [19] Xiao-Gang Wen: *Quantum Field Theory of Many-Body Systems*, Oxford University Press (2004).
- [20] Y. Ben Tov: "Schwinger-Keldysh path integral for the quantum harmonic oscillator", arXiv:2102.05029.

- [21] P. Woit: *Quantum Theory, Groups and Representations. An Introduction*, Springer, Cham (2017).
- [22] P. A. Horvathy: “The Maslov correction in the semiclassical Feynman integral”, *Central Eur. J. Phys.* **9** (2011), 1 [arXiv:quant-ph/0702236].
- [23] Ph. Pechukas: “Time-dependent semiclassical scattering theory. I. Potential scattering”, *Phys. Rev.* **181** (1969) 166.
- [24] K. Osterwalder and R. Schrader: ”Axioms for euclidean Green’s functions”, *Comm. Math. Phys.* **31** (1973), 83 - 112; **42** (1975), 281 – 305.
- [25] R. A. Horn and Ch, R. Johnson: *Matrix analysis*, Cambridge University Press, 21st printing, New York (2007).
- [26] A. Balaž, I. Vidanović, A. Bogojević, A. Belić, and A. Pelster: ”Fast converging path integrals for time-dependent potentials I: Recursive calculation of short-time expansion of the propagator”, *J. Stat. Mech.* P03004 (2011), [arXiv:0912.2743].
- [27] A. Balaž, I. Vidanović, A. Bogojević, A. Belić and A. Pelster: ”Fast converging path integrals for time-dependent potentials II: Generalization to many-body systems and real-time formalism”, *J. Stat. Mech.* 1103 (2011) P03005 [arXiv:1011.5185].
- [28] A. Boriçi and R. Rosenfelder: “Scaling in SU(3) theory with a MCRG improved lattice action”, *Nucl. Phys. Proc. Suppl.* **63** (1998), 925 – 927 [arXiv:hep-lat/9711035].
- [29] J. M. Pérez-Jordá, E. San-Fabián and F. Moscardó: ”A simple, reliable and efficient scheme for automatic numerical integration”, *Comp. Phys. Comm.* **70** (1992) 271–284.
- [30] G. P. Lepage: ”A new algorithm for adaptive multidimensional integration”, *J. Comp. Phys.* **27** (1978), 192.
- [31] P. Vivo: ”Index of a matrix, complex logarithms, and multidimensional Fresnel integrals”, arXiv:2011.12007 [cond-mat.stat-mech].
- [32] R. Rosenfelder: “Path Integrals for Potential Scattering”, *Phys. Rev. A* **79** (2009), 012701 [arXiv:0806.3217 [nucl-th]]
- [33] R. Rosenfelder: ”Scattering Theory with Path Integrals”, *J. Math. Phys.* **55** (2014), 032106 [arXiv:1302.3419[nucl-th]].
- [34] H. J. Rothe: *Lattice gauge theories. An introduction*, 3rd edition, World Scientific Lecture Notes in Physics – vol. 74, World Scientific, New Jersey (2005).
- [35] https://en.wikipedia.org/wiki/Recurrence_relation.
- [36] M. Abramowitz and I. Stegun (eds.): *Handbook of Mathematical Functions*, Dover, New York (1965).
- [37] I. S. Gradshteyn and I. M. Ryzhik: *Table of Integrals, Series, and Products*, 4th edition, Academic Press, New York (1980).